

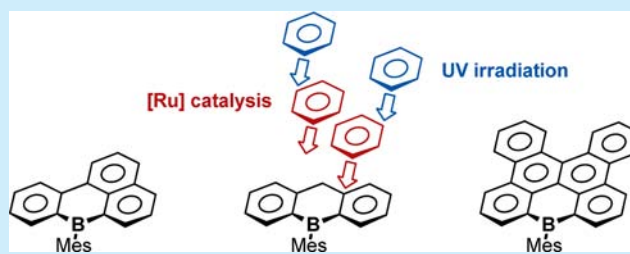
## Ru-Catalyzed Benzannulation Leads to Luminescent Boron-Containing Polycyclic Aromatic Hydrocarbons

Valentin M. Hertz, Hans-Wolfram Lerner, and Matthias Wagner\*

Institut für Anorganische Chemie, Goethe-Universität Frankfurt, Max-von-Laue-Strasse 7, 60438 Frankfurt (Main), Germany

## Supporting Information

**ABSTRACT:** A series of boron-containing polycyclic aromatic hydrocarbons (PAHs) have been synthesized through the Ru-catalyzed cyclization of aryl ene-yne. The benchtop-stable products show deep blue photoluminescence. Reversible electrochemical reduction is possible at moderate electrode potentials (about  $-2.0$  V vs FcH/FcH<sup>+</sup>); some of the compounds also underwent reversible oxidation. The systematic expansion of the PAH scaffolds permitted the analysis of even subtle structure–property relationships.



Recent rapid progress in organic optoelectronics was sparked by the discovery of graphene and is fueled by the development of novel, efficient tools for the preparation of tailor-made polycyclic aromatic hydrocarbons (PAHs, nanographenes). Tailoring PAHs for specific applications requires the adjustment of their frontier orbital energy levels and, in turn, their light absorption/emission characteristics and electron-accepting capacities. This can be achieved by varying the sizes or the substituents of the  $\pi$  systems. Another approach uses substitutional doping, that is, replacement of selected carbon atoms within a  $\pi$ -conjugated framework by other main-group atoms.<sup>1,2</sup>

Among the possible dopant elements, N, P, and S possess electron lone pairs and lead, after partial oxidation, to p-type materials. Boron atoms are the ideal counterparts of N, P, and S for the preparation of complementary n-type materials: overlap of the vacant boron p orbital with adjacent  $\pi$ -electron clouds not only facilitates electron injection but also tends to shift the fluorescence wavelengths into the visible region of the spectrum. Contrary to the established chemistry of p-type organic semiconductors, their B-doped congeners are far less well developed, mainly due to synthetic challenges associated with the handling of air- and moisture-sensitive organoboron intermediates.<sup>2,3</sup> These challenges can be met by introducing the boron atom in the last step of the synthesis sequence. More versatile approaches start from already boron-containing building blocks. In these cases, however, the dopant atoms have to be sterically protected to tolerate subsequent functionalization reactions, such as Buchwald–Hartwig,<sup>4</sup> Negishi,<sup>5,6</sup> Sonogashira,<sup>7–9</sup> Stille,<sup>10–13</sup> or Suzuki coupling protocols.<sup>14,15</sup> All transformations mentioned were aimed at the peripheral derivatization of already preformed triarylboranes. In contrast, metal-mediated reactions contributing to the actual assembly of a B-containing PAH framework are extremely scarce. As a prominent example, Yamaguchi et al. used stoichiometric FeCl<sub>3</sub> in a Scholl-type reaction to convert a 6,13-di(9-anthryl)-6,13-dihydro-6,13-

diborapentacene into the corresponding, fully planarized nanographene.<sup>16</sup>

Herein, we apply Ru-catalyzed (double) cyclization reactions<sup>17–19</sup> to annulate new benzene rings onto pre-existing arylboranes and -silanes (Figure 1). The actual choice of starting

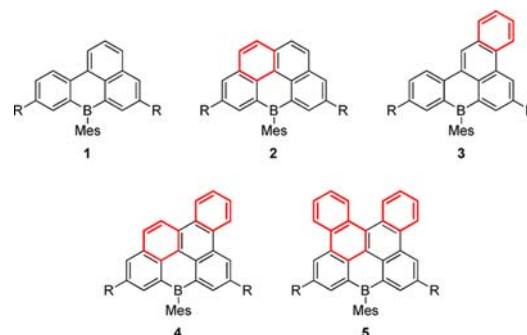


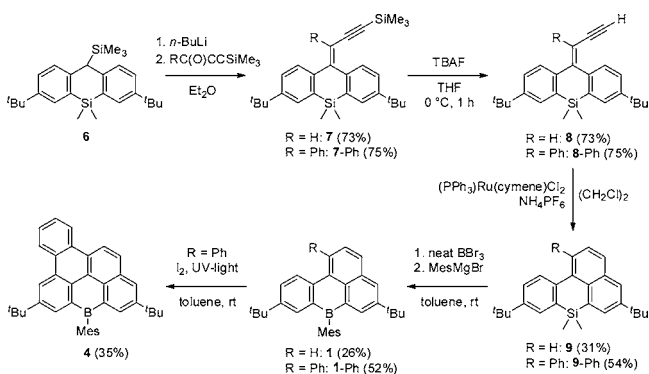
**Figure 1.** Polycyclic conjugated arylboranes with  $\pi$  systems of different sizes and shapes; R = *tert*-butyl.

materials (6 vs 10; Schemes 1 and 2) had to take into account that Si/B exchange on highly rigid molecular scaffolds either requires forcing conditions or fails completely (cf. the synthesis of 5<sup>20</sup>). Fortunately, whenever necessary, our highly modular synthesis sequence enables us to introduce the boron atom already at an earlier stage (cf. 9-Ph  $\rightarrow$  1-Ph  $\rightarrow$  4; synthesis of 2 from 10). Moreover, we can systematically vary the numbers and positions of benzene rings fused to a given arylborane lead structure (Figure 1) and thereby assess key structure–property relationships.

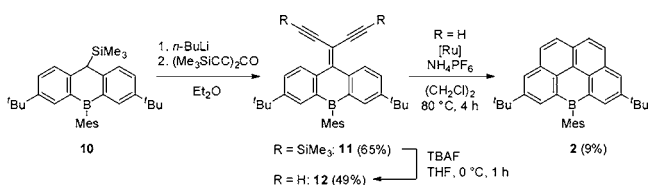
A key reaction step, common to all syntheses described in Schemes 1 and 2, is the Peterson olefination reaction between the

Received: September 9, 2015

Published: October 15, 2015

Scheme 1. Synthesis of 1, 1-Ph, and 4 from 6<sup>a</sup>

<sup>a</sup>Yields are given relative to **6**.

Scheme 2. Synthesis of 2 from 10<sup>a</sup>

<sup>a</sup>Silyl substituents were removed from **11** before reaction with [Ru] = (PPh<sub>3</sub>)Ru(cymene)Cl<sub>2</sub>. Yields are given relative to **10**.

B/Si heterocycles<sup>20</sup> **6/10** and alkyne ketones. At the next stage, the obtained alkyne intermediates **7**, **7-Ph**, and **11** were deprotected with [*n*-Bu<sub>4</sub>N]F (TBAF) because the Ru-catalyzed annulation process necessarily requires terminal alkynes as substrates.<sup>17,18</sup> All the deprotected alkynes **8**, **8-Ph**, and **12** are sufficiently stable to withstand chromatographic workup. Nevertheless, the free ene-diyne **12** should ideally be used without delay for further reactions or otherwise stored at low temperatures (−30 °C). Cyclization can be performed once to furnish **9/9-Ph** (Scheme 1) or twice to afford **2** (Scheme 2).

The reaction can be carried out either in a microwave reactor or in a Schlenk vessel (1,2-dichloroethane, 75–84 °C, 3–4 h). When working with small amounts, we found it convenient to use the microwave reactor. The preparation of larger batches in Schlenk vessels gives slightly better yields compared to microwave conditions, likely because the substrate can be added dropwise over an extended period of time. Si/B exchange was achieved by treating **9/9-Ph** with excess neat BBr<sub>3</sub> at room temperature; after evaporation of residual BBr<sub>3</sub>, the crude product was mesitylated without further purification (**1/1-Ph**).<sup>21</sup> As the dangling phenyl ring in **1-Ph** is part of a stilbene-type substructure, the molecule readily undergoes a light-induced conversion to the fully planarized **4** upon irradiation with a Hg medium-pressure lamp; related photocyclization reactions have recently been reported by us for the synthesis of boron-bridged 9-phenylphenanthrenes and dibenzo[*g,p*]chrysenes, such as **3** and **5** (Figure 1).<sup>20</sup> All of the B-containing PAHs proved to be benchtop-stable and could be purified by column chromatography on silica gel.

Compounds **1/1-Ph**, **2-4**, **7/7-Ph**, **9/9-Ph**, and **11** were fully characterized by <sup>1</sup>H, <sup>11</sup>B{<sup>1</sup>H}/<sup>29</sup>Si-INEPT, and <sup>13</sup>C{<sup>1</sup>H} NMR spectroscopy as well as HRMS and elemental analysis. In the cases of the alkyne intermediates **8/8-Ph** and **12**, deprotection was confirmed to be complete by proton NMR spectroscopy; singlet resonances at about 3.2 ppm are diagnostic for these

terminal alkynes. Upon successful cyclization, all alkyne resonances vanished and new signals appeared in the aromatic region. Si/B exchange on **9** and **9-Ph** resulted in significant downfield shifts of the CH carbon resonances in *o*- and *p*-positions of the heteroatoms (up to Δδ = 9 ppm). The <sup>11</sup>B NMR signals of all target boranes are severely broadened, with chemical shift values of approximately 65 ppm.

The electrochemical properties of **1–5** were investigated by cyclic voltammetry (Figure 2; CH<sub>2</sub>Cl<sub>2</sub>, 0.1 M [*n*-Bu<sub>4</sub>N][PF<sub>6</sub>], vs

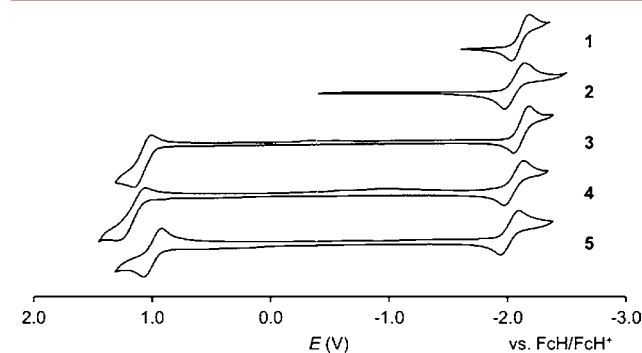


Figure 2. Cyclic voltammograms of **1–5** measured in CH<sub>2</sub>Cl<sub>2</sub>.

FcH/FcH<sup>+</sup>). Even for the smallest PAH of the series (**1**), we observed a reversible redox event at a moderately cathodic potential value of  $E_{1/2} = -2.11$  V. Annulation of further benzene rings has surprisingly little effect on the reduction potentials of the respective compounds **2–5** (Table 1 and Figure 2). A totally different picture is revealed for the anodic scan: even though the oxidation of all five compounds starts at similar onset potentials of approximately 1 V, only the PAHs **3** (five six-membered rings) and **5** (seven six-membered rings) show reversible behavior ( $E_{1/2} = 1.09$  and 1.00 V, respectively). Electron removal from compound **4** (six six-membered rings) is only partially reversible. This is a remarkable result because the shape of an actual PAH seems to be more important for its electronic properties (cf. **2** vs **3**) than the mere size of the  $\pi$  system (cf. **3** vs **4** or **5**).

Compound **1** can be regarded as a boron-bridged 1-phenylnaphthalene. In the UV/vis absorption spectrum, 1-phenylnaphthalene (**A**) shows a longest-wavelength absorption maximum ( $\lambda_{\text{abs}}$ ) at 290 nm (Figure 3).<sup>22</sup> Planarization of the molecular framework, enforced by a methylene bridge, results in a moderate bathochromic shift of 45 nm (benzo[*c*]fluorene (**B**):  $\lambda_{\text{abs}} = 335$  nm).<sup>23</sup> The absorption maximum of the boron-bridged species **1** is shifted by an additional 74 nm to  $\lambda_{\text{abs}} = 409$  nm (Table 1 and Figure 3), thereby testifying to a pronounced influence of the vacant boron p orbital on the electronic structure of the  $\pi$ -electron system. The extended compound **3** ( $\lambda_{\text{abs}} = 408$  nm) has a UV/vis spectrum very similar to that of **1**. Compared to these two compounds, the absorption maxima of the remaining PAHs, **2**, **4**, and **5**, are bathochromically shifted and appear in the narrow range between 424 and 429 nm. We therefore conclude that benzannulation at a bay region (**1** → **2** or **3** → **4**) influences the absorption properties to a larger extent than benzannulation at the periphery of the PAH (**1** → **3**, **2** → **4**, or **4** → **5**). In the emission spectra (C<sub>6</sub>H<sub>12</sub>), vibrational fine structures were observed for **1–5**. The individual emission maxima are especially well-resolved in the case of **2** (Figure 4), thereby indicating a particularly rigid scaffold. PAHs **1–5** emit in the visible, deep blue spectral region (shortest-wavelength emission maxima:  $\lambda_{\text{em}} = 420$ –439 nm, Figure 3). In contrast,

Table 1. Photophysical and Electrochemical Properties of 1–5 and 1-Ph

compd	$\lambda_{\text{abs}}$ (nm) ( $\epsilon$ , $M^{-1} \text{ cm}^{-1}$ )	$\lambda_{\text{onset}}^a$ (nm)	$\lambda_{\text{ex}}$ (nm)	$\lambda_{\text{em}}$ (nm)	$\Phi_{\text{PL}}^b$ (%)	Stokes shift ( $\text{cm}^{-1}$ ) <sup>c</sup>	$E_{\text{HOMO}}/E_{\text{LUMO}}^d$ (eV)	$E_{1/2}$ (V)	$E_{\text{G}}^{\text{CV}}$ (eV) <sup>e</sup>	$E_{\text{G}}^{\text{opt}}$ (eV) <sup>f</sup>
1	395 (13000)	431	390	431	80	1248	–/–2.69	–2.11		2.88
	409 (11000)			450						
2	392 (11300)	435	392	430	79	163	–/–2.74	–2.06		2.85
	404 (11000)			456						
	427 (13000)			486						
3	388 (19000)	420	380	420	83	700	–5.89/–2.69	–2.11	3.20	2.95
	408 (28800)			443				1.09		
4	395 (17200)	439	390	433	72	490	–/–2.75	–2.05		2.82
	404 (18800)			456				1.18 <sup>g</sup>		
	424 (14500)									
5	407 (14000)	441	400	439	70	531	–5.80/–2.79	–2.01	3.01	2.81
	429 (22000)			465				1.00		
1-Ph	406 (14400)	441	395	470	91	3354	–/–2.65	–2.15		2.81

<sup>a</sup>Onset wavelengths ( $\lambda_{\text{onset}}$ ) were determined by constructing a tangent at the point of inflection of the bathochromic slope of the most red-shifted absorption maximum. <sup>b</sup>Quantum yields were determined using a calibrated integrating sphere. <sup>c</sup>Stokes shifts represent the difference between each longest-wavelength absorption maximum and the corresponding shortest-wavelength emission maximum. <sup>d</sup> $E_{\text{HOMO}} = -4.8 \text{ eV} - E_{1/2}^{\text{Ox}}$ ,  $E_{\text{LUMO}} = -4.8 \text{ eV} - E_{1/2}^{\text{Red}}$  ( $\text{FcH}/\text{FcH}^+ = -4.8 \text{ eV}$  vs vacuum level). <sup>e</sup>Electrochemically determined band gap. <sup>f</sup>Optical band gap  $E_{\text{G}}^{\text{opt}} = 1240/\lambda_{\text{onset}}$ . <sup>g</sup>Not completely reversible.

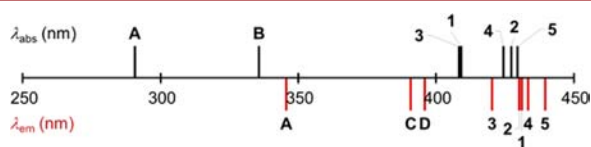


Figure 3. Longest-wavelength UV/vis absorption maxima and emission maxima of 1–5 and of some PAHs selected for comparison (A, 1-phenylnaphthalene; B, benzo[*c*]fluorene; C, [4]helicene; D, dibenzo[*g,p*]chrysene).

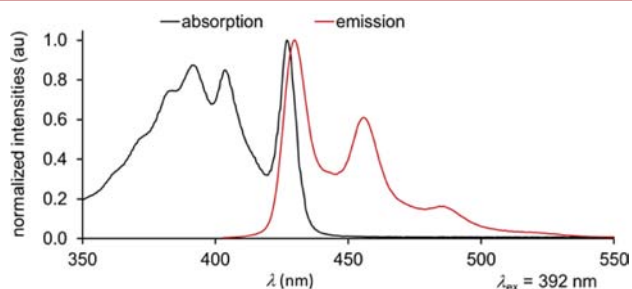


Figure 4. UV/vis absorption and emission spectrum of 2 measured in  $\text{C}_6\text{H}_{12}$ .

their all-carbon relatives 1-phenylnaphthalene (A), [4]helicene (C), and dibenzo[*g,p*]chrysene (D) exhibit broad fluorescence bands at 345,<sup>24</sup> 390,<sup>24</sup> and 395 nm,<sup>25</sup> respectively. Thus, by integration of a boron atom into the smallest parent system, 1-phenylnaphthalene, we changed the emission characteristics to a much larger extent (>85 nm) than by our subsequent modifications of the size and shape of the  $\pi$  system (<20 nm). The photoluminescence quantum efficiencies of 1–5 are high and fall into the range of  $\Phi_{\text{PL}} = 70$ –83%. Remarkably, attachment of a phenyl ring to 1 increases  $\Phi_{\text{PL}}$  from 80 to 91% (1-Ph, Table 1).

In summary, we succeeded in the synthesis of a series of novel boron-doped PAHs, which are inert toward air and moisture, electrochemically well-behaved, and highly luminescent in the blue spectral region. A key step of the synthesis sequence employs the Ru-catalyzed cyclization of ene-yne to annulate new benzene rings onto pre-existing aryl scaffolds. Hereby, we

introduced this transition-metal-mediated reaction for the late-stage transformation of arylboranes and -silanes. By combining a Peterson olefination with Ru-catalyzed and/or photoinduced cyclization reactions, we developed a highly modular approach to vary and expand a chosen lead structure in a systematic manner. These results should provide a useful guideline for the future targeted design of boron-containing PAH luminophores.

## ■ ASSOCIATED CONTENT

### Supporting Information

The Supporting Information is available free of charge on the ACS Publications website at DOI: 10.1021/acs.orglett.5b02604.

Experimental procedures and NMR data/spectra for all new compounds, UV/vis absorption and emission spectra, and cyclic voltammograms of 1–4 (PDF)

## ■ AUTHOR INFORMATION

### Corresponding Author

\*E-mail: matthias.wagner@chemie.uni-frankfurt.de.

### Notes

The authors declare no competing financial interest.

## ■ ACKNOWLEDGMENTS

This work was supported by the Goethe-Universität Frankfurt.

## ■ REFERENCES

- (1) Dral, P. O.; Kivala, M.; Clark, T. *J. Org. Chem.* **2013**, *78*, 1894–1902.
- (2) (a) Entwistle, C. D.; Marder, T. B. *Angew. Chem., Int. Ed.* **2002**, *41*, 2927–2931. (b) Yamaguchi, S.; Wakamiya, A. *Pure Appl. Chem.* **2006**, *78*, 1413–1424. (c) Jäkle, F. *Chem. Rev.* **2010**, *110*, 3985–4022. (d) Rao, Y.-L.; Amarné, H.; Wang, S. *Coord. Chem. Rev.* **2012**, *256*, 759–770. (e) Lorbach, A.; Hübner, A.; Wagner, M. *Dalton Trans.* **2012**, *41*, 6048–6063. (f) Escande, A.; Ingleson, M. J. *Chem. Commun.* **2015**, *51*, 6257–6274.
- (3) Narita, A.; Wang, X. Y.; Feng, X.; Müllen, K. *Chem. Soc. Rev.* **2015**, *44*, 6616–6643.
- (4) Numata, M.; Yasuda, T.; Adachi, C. *Chem. Commun.* **2015**, *51*, 9443–9446.

- (5) Liu, X. Y.; Bai, D. R.; Wang, S. *Angew. Chem., Int. Ed.* **2006**, *45*, 5475–5478.
- (6) Hudson, Z. M.; Liu, X.-Y.; Wang, S. *Org. Lett.* **2011**, *13*, 300–303.
- (7) Yamaguchi, S.; Shirasaka, T.; Tamao, K. *Org. Lett.* **2000**, *2*, 4129–4132.
- (8) Collings, J. C.; Poon, S.-Y.; Le Droumaguet, C.; Charlot, M.; Katan, C.; Pålsson, L.-O.; Beeby, A.; Mosely, J. A.; Kaiser, H. M.; Kaufmann, D.; Wong, W.-Y.; Blanchard-Desce, M.; Marder, T. B. *Chem. - Eur. J.* **2009**, *15*, 198–208.
- (9) Sun, C.; Lu, J.; Wang, S. *Org. Lett.* **2011**, *13*, 1226–1229.
- (10) Reus, C.; Weidlich, S.; Bolte, M.; Lerner, H.-W.; Wagner, M. *J. Am. Chem. Soc.* **2013**, *135*, 12892–12907.
- (11) Reus, C.; Guo, F.; John, A.; Winhold, M.; Lerner, H.-W.; Jäkle, F.; Wagner, M. *Macromolecules* **2014**, *47*, 3727–3735.
- (12) Guo, F.; Yin, X.; Pammer, F.; Cheng, F.; Fernandez, D.; Lalancette, R. A.; Jäkle, F. *Macromolecules* **2014**, *47*, 7831–7841.
- (13) Cheng, F.; Bonder, E. M.; Jäkle, F. *J. Am. Chem. Soc.* **2013**, *135*, 17286–17289.
- (14) Crawford, A. G.; Liu, Z.; Mkhaliid, I. A. I.; Thibault, M.-H.; Schwarz, N.; Alcaraz, G.; Steffen, A.; Collings, J. C.; Batsanov, A. S.; Howard, J. A. K.; Marder, T. B. *Chem. - Eur. J.* **2012**, *18*, 5022–5035.
- (15) Matsuo, K.; Saito, S.; Yamaguchi, S. *J. Am. Chem. Soc.* **2014**, *136*, 12580–12583.
- (16) (a) Dou, C.; Saito, S.; Matsuo, K.; Hisaki, I.; Yamaguchi, S. *Angew. Chem., Int. Ed.* **2012**, *51*, 12206–12210. (b) A ring-closing metathesis strategy has been used to prepare 1,2-dihydro-1,2-azaborine: Marwitz, A. J. V.; Matus, M. H.; Zakharov, L. N.; Dixon, D. A.; Liu, S.-Y. *Angew. Chem., Int. Ed.* **2009**, *48*, 973–977.
- (17) Merlic, C. A.; Pauly, M. E. *J. Am. Chem. Soc.* **1996**, *118*, 11319–11320.
- (18) Donovan, P. M.; Scott, L. T. *J. Am. Chem. Soc.* **2004**, *126*, 3108–3112. Similar to the synthesis protocols described therein, we usually employed 0.15 equiv of Ru catalyst per triple bond.
- (19) Shen, H.-C.; Tang, J.-M.; Chang, H.-K.; Yang, C.-W.; Liu, R.-S. *J. Org. Chem.* **2005**, *70*, 10113–10116.
- (20) Hertz, V. M.; Bolte, M.; Lerner, H.-W.; Wagner, M. *Angew. Chem., Int. Ed.* **2015**, *54*, 8800–8804.
- (21) Gabbai et al. obtained a partially fluorinated derivative of **1** in 17% isolated yield by nucleophilic substitution of  $(C_6F_5)_2BF \cdot Et_2O$  with 1,8-dilithionaphthalene-tmeda: Schulte, M.; Gabbai, F. P. *J. Organomet. Chem.* **2002**, *643–644*, 164–167.
- (22) Friedel, R. A.; Orchin, M.; Reggel, L. *J. Am. Chem. Soc.* **1948**, *70*, 199–204.
- (23) Jacobs, W. A.; Craig, L. C.; Lavin, G. I. *J. Biol. Chem.* **1941**, *141*, 51–66.
- (24) Berlman, I. B. *Fluorescence Spectra of Aromatic Molecules*, 2nd ed.; Academic Press: New York, 1971.
- (25) Hashimoto, S.; Ikuta, T.; Shiren, K.; Nakatsuka, S.; Ni, J.; Nakamura, M.; Hatakeyama, T. *Chem. Mater.* **2014**, *26*, 6265–6271.